

## A new adaptive algorithm for reducing non-linear effects from saturation in active noise control systems

Márcio H. Costa<sup>1,†</sup> and José Carlos M. Bermudez<sup>2,\*‡</sup>

<sup>1</sup>*Escola de Engenharia e Arquitetura, Universidade Católica de Pelotas, 96010-000 Pelotas, RS, Brazil*

<sup>2</sup>*Department of Electrical Engineering, Federal University of Santa Catarina, 88040-900 Florianópolis, SC, Brazil*

### SUMMARY

Adaptive algorithms applied to active noise and vibration control are frequently designed for maximum performance in linear environments. In many cases, non-linear effects can severely impair the adaptive algorithm performance. One of the most common non-linear effects is saturation, which can occur at the electronic circuits that drive the acoustic or mechanical transducers. An effective solution to mitigate such non-linear distortions is to embed an automatic control of the non-linear effects within the adaptive algorithm. Algorithms that use this approach are called minimum effort adaptive filters. This work presents a new minimum effort algorithm (MOV-FXLMS), based on the minimum output variance least mean square estimator, for situations in which the influence of the secondary path cannot be neglected and its output is constrained by a saturation non-linearity. Analytical expressions are obtained for the behaviour of the mean weight vector and for the mean square error for Gaussian inputs and slow learning. Monte Carlo simulations show excellent agreement with the predictions of the theoretical model. The optimum penalty factor (a design parameter of the MOV-FXLMS algorithm) is determined as a function of the system's degree of non-linearity. The new algorithm provides an unbiased solution to the associated non-linear mean square estimation problem for small estimation errors of the secondary path and degree of non-linearity. Robustness of the algorithm's performance to such errors is addressed. The new algorithm is compared with the conventional FXLMS algorithm for performance. Copyright © 2004 John Wiley & Sons, Ltd.

KEY WORDS: adaptive filtering; active noise control; FXLMS

### 1. INTRODUCTION

Active systems, designed for sound or vibration control, employ adaptive filters to generate the signals required to interfere destructively with the field caused by the original source of

---

\*Correspondence to: J. C. M. Bermudez, Department of Electrical Engineering, Federal University of Santa Catarina, 88040-900, Florianópolis, SC, Brazil.

†E-mail: j.bermudez@ieec.org

‡E-mail: m.costa@ieec.org

Contract/grant sponsor: Conselho Nacional de Desenvolvimento Científico e Tecnológico - CNPq  
Contract/grant sponsor: Fundação de Amparo à Pesquisa do Rio Grande do Sul – FAPERGS

disturbance [1–3]. Active noise control (ANC) systems are usually implemented by feedforward structures which, for the single channel case, consist of a reference sensor at the primary source of disturbance, a secondary source for the destructive interference, an error sensor, and an adaptive controller. Sensors can be microphones (sound control), piezoelectric transducers or accelerometers (vibration control). Secondary sources can be speakers (sound) or piezoelectric transducers (vibration). Multiple channel systems have multiple sensors and actuators whose outputs are combined in some meaningful cost function to be optimized.

The most employed adaptive algorithm in ANC is the filtered-X LMS algorithm (FXLMS) [1]. The FXLMS algorithm is a modified version of the least mean squares (LMS) algorithm, in which the reference signal is filtered to compensate for filtering operations in the electroacoustic adaptation loop (the so-called secondary path).

Proper design of adaptive systems requires the modelling of the adaptive algorithm's behaviour under the conditions dictated by the specific application. Most adaptive system analyses neglect non-linear effects and model the unknown systems as linear with memory. In many important practical circumstances, a linear model simplifies the mathematics and permits detailed system analysis. More sophisticated models, however, must be used when non-linear effects significantly impact upon actual system behaviour [4–8]. Important non-linear effects occur in ANC systems [7]. Sound and vibration control systems include acoustical or mechanical paths. Signal converters (A/D and D/A), power amplifiers and transducers (speakers or actuators) can non-linearly transform digital electrical signals into analog electrical or mechanical signals. This non-linear effect is frequently caused by overdriving the electronics or the transducers in the secondary path [9,10]. In these cases, non-linearities can be adequately modelled by a saturation function.

Reference [5] recently studied the statistical behaviour of the FXLMS algorithm for a memoryless non-linear secondary path. Saturation non-linearities were shown to significantly affect algorithm performance. The possibility of quantifying the non-linear effects on the performance surface and on the adaptive algorithm behaviour motivated the search for new algorithms that could be capable of improving steady-state performance of the FXLMS algorithm in a non-linear environment. Such a solution would allow the use of cheaper amplifiers and transducers without a significant performance loss, therefore reducing implementation costs.

One solution to avoid such non-linear distortions is to overdesign the system, which usually increases the cost and limits the system's performance. A more effective solution is to embed an automatic control of the non-linear effects within the adaptive algorithm. This is usually achieved by adding a penalty function to the adaptive algorithm's cost function in order to control the signal amplitude at the non-linearity input. Algorithms that use this approach are called minimum effort adaptive filters [11–16]. Two important examples are the Leaky-LMS [12], which seeks to minimize the norm of the filter's tap weight vector, and the minimum output variance least mean square adaptive estimator (MOV-LMS) [11,13–16], which minimizes the adaptive filter output power. From these, the MOV-LMS is the most appropriate to handle saturation non-linearities at the adaptive filter output, as it directly controls the power at the non-linearity input.

The complexity of the MOV-LMS algorithm is of the same order as the LMS algorithm. It requires only one more extra scalar multiplication and one extra subtraction, as compared to LMS. The behaviours of the Leaky-LMS and MOV-LMS algorithms have been analysed for linear systems [11,12]. The behaviour of the MOV-LMS for non-linear secondary paths has been

analysed in Reference [13]. In this analysis, filtering effects in the secondary path were neglected. It has been shown that the mean weight vector converges to the linear Wiener solution multiplied by a real scalar (multiplicative bias). It has also been shown that the MOV-LMS algorithm can reach the minimum of the MSE performance surface for the non-linear case if its penalty factor is properly designed. The results obtained in Reference [13], however, cannot be directly applied to ANC systems when the effects of the linear filtering in the secondary path must be considered. In this case, the adaptive algorithm typically employed is the FXLMS algorithm.

This work proposes the MOV-FXLMS algorithm for use in systems where the adaptive filter is followed by a linear filtering operation and a saturation non-linearity.<sup>§</sup> The MOV-FXLMS algorithm controls the signal power at the non-linearity's input. A statistical analysis of the algorithm is presented. Analytical expressions are obtained for the transient and steady-state mean weight and MSE behaviours for Gaussian inputs and slow learning. Monte Carlo simulations show excellent agreement between algorithm behaviour and theoretical predictions. The optimum penalty factor is determined, which leads to an unbiased converged mean weight vector.<sup>¶</sup> Thus, it is shown that the MOV-FXLMS algorithm can also reach the minimum of the MSE surface if properly designed. Since the optimum penalty factor is a function of the system's degree of non-linearity, the robustness of the algorithm's performance to errors in its estimation is also addressed. It is shown that the MOV-FXLMS algorithm is robust to such estimation errors. The MOV-FXLMS and the FXLMS algorithms are compared for performance. It is shown that the MOV-FXLMS algorithm provides much better steady-state performance for moderate and large degrees of non-linearity.

## 2. THE SYSTEM MODEL

Figure 1 shows a block diagram of the adaptive system considered. It is assumed that the desired signal  $d(n)$  is linearly related to the input signal  $x(n)$  according to

$$d(n) = \sum_{k=0}^{N-1} w_k^o x(n-k) + z(n) \quad (1)$$

which can be expressed in vector form as

$$d(n) = \mathbf{W}^o \mathbf{X}(n) + z(n) \quad (2)$$

where  $\mathbf{W}^o = [w_0^o \ w_1^o \ \dots \ w_{N-1}^o]^T$  is the vector of model parameters and  $\mathbf{X}(n) = [x(n) \ x(n-1) \ \dots \ x(n-N+1)]^T$  is the observed data vector. The random sequence  $\{z(n)\}$  is assumed independent, identically distributed (i.i.d.), stationary, zero-mean Gaussian with variance  $\sigma_z^2$ , and statistically independent of the random input sequence  $\{x(n)\}$ .  $z(n)$  accounts for

<sup>§</sup>The linear filtering represents the subsystem responses (linear effects in amplifiers and transducers) that precede the saturation non-linearity. The remaining part of the secondary path, from the saturation non-linearity to the error sensor, is considered ideal. This structure takes into consideration the linear filtering that affects the input to the non-linearity (the main concern in the non-linear case) while keeping the mathematical analysis manageable. The model is more accurate as the actuators (speakers in ANC) get physically closer to the sensors (microphones in ANC).

<sup>¶</sup>The mean weight vector converges to the weight vector at the minimum of the performance surface for the linear case [17].

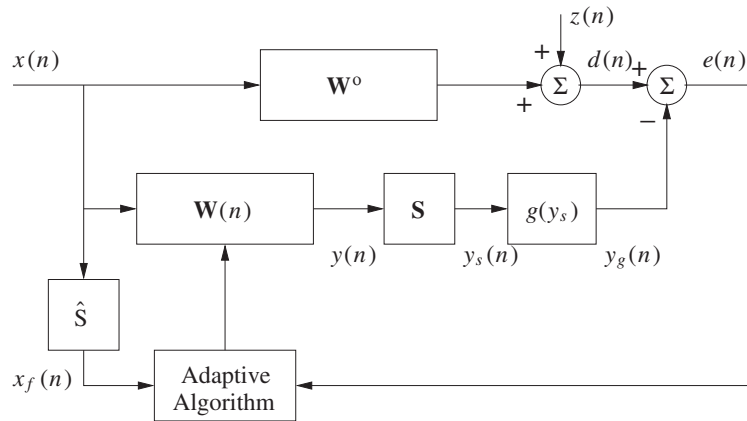


Figure 1. Block diagram of the non-linear adaptive system.

measurement noise and modelling errors in (1).  $\mathbf{W}(n) = [w_0(n) \ w_1(n) \ \cdots \ w_{N-1}(n)]^T$  is the adaptive weight vector.  $\mathbf{S} = [s_0 \ s_1 \ \cdots \ s_{M-1}]^T$  is the secondary path response and  $\hat{\mathbf{S}} = [\hat{s}_0 \ \hat{s}_1 \ \cdots \ \hat{s}_{M-1}]^T$  is the estimate of the secondary path response. The input sequence  $\{x(n)\}$  is assumed to be a zero-mean wide sense stationary Gaussian process with variance  $\sigma_x^2$ .  $x_f(n)$  is the filtered signal and  $\mathbf{X}_f = [x_f(n) \ x_f(n-1) \ \cdots \ x_f(n-N+1)]^T$  is the filtered input data vector.  $y(n)$  is the output of the adaptive filter;  $y_s(n)$  is the output of the linear filter  $\mathbf{S}$ ;  $g(\cdot)$  is the saturation non-linearity;  $y_g(n)$  is the non-linearity output and  $e(n)$  is the error signal. The saturation non-linearity is modelled by the scaled error function

$$g(y) = \int_0^y e^{-\frac{\psi^2}{2\sigma^2}} d\psi \tag{3}$$

This model is frequently used in analyses of saturation effects [13,18,19]. Note that  $\lim_{\sigma^2 \rightarrow \infty} [g(y)] = y$  and  $\lim_{\sigma^2 \rightarrow 0} [g(y)] = \sigma \sqrt{(\pi/2)} \operatorname{sgn}(y)$ . Hence, by changing  $\sigma^2$ ,  $g(y)$  can be varied between a linear device and a hard limiter.  $g(y)$  models a saturation type non-linearity that is of great practical interest. Different values of  $\sigma$  in (3) lead to different saturation levels. The effects of very large non-linearities ( $\sigma \rightarrow 0$ ) with a fixed saturation level can be studied by scaling  $g(y)$  by a constant such as  $A/\sigma$ ,  $A \in \mathbb{R}^+$ . In this case,  $\max\{y_g^2(n)\} = (\pi/2)A^2$ . In this work, we study the effects of the non-linearity  $g(y)$  in (3). The effects of a fixed saturation level non-linearity can be easily determined by including the scaling factor  $A/\sigma$  in the expressions derived here.

### 3. DERIVATION OF THE MOV-FXLMS ALGORITHM

Using the minimum output variance criterion [11,13,14], we are interested in controlling the variance of the signal at the non-linearity input (output of the filter  $\mathbf{S}$ ) while minimizing the mean square error. We consider initially the case of a purely linear secondary path. This

facilitates the derivation of a simple update equation that controls the power at the non-linearity input. We then analyse the behaviour of the derived algorithm in the non-linear setting and determine the optimal value of its control parameter (penalty factor) in order to avoid a biased solution.

Consider the following cost function to be minimized, which penalizes any increase in the signal power at the output of  $\mathbf{S}$  [11,13,14]:

$$J(n) = e^2(n) + \gamma y_s^2(n) \quad (4)$$

where  $\gamma$  is known as the effort penalty factor [14] and

$$y_s(n) = \sum_{i=0}^{M-1} s_i \mathbf{W}^T(n-i) \mathbf{X}(n-i) \quad (5)$$

is the output of the adaptive filter. The error signal is given by

$$e(n) = \mathbf{W}^o T \mathbf{X}(n) + z(n) - \sum_{i=0}^{M-1} s_i \mathbf{W}^T(n-i) \mathbf{X}(n-i) \quad (6)$$

which is a function of  $\mathbf{W}(n-i)$ ,  $i = 0, \dots, M-1$ . Following the stochastic gradient approach, we define the weight update equation

$$\mathbf{W}(n+1) = \mathbf{W}(n) - \frac{\mu}{2} \sum_{j=0}^{M-1} \frac{\partial J(n)}{\partial \mathbf{W}(n-j)} \quad (7)$$

The updating term in (7) is calculated in Appendix A, yielding the following weight update equation for the MOV-FXLMS algorithm:

$$\mathbf{W}(n+1) = \mathbf{W}(n) + \mu[e(n) - \gamma \hat{y}_s(n)] \mathbf{X}_f(n) \quad (8)$$

where

$$\mathbf{X}_f(n) = \sum_{j=0}^{\hat{M}-1} \hat{s}_j \mathbf{X}(n-j) \quad (9)$$

is the filtered input signal vector and

$$\hat{y}_s(n) = \sum_{i=0}^{\hat{M}-1} \hat{s}_i \mathbf{W}^T(n-i) \mathbf{X}(n-i) \quad (10)$$

is an estimate of the non-linearity input, based on the coefficients of the estimated secondary path response  $\hat{\mathbf{S}}$ .

#### 4. THE MEAN WEIGHT BEHAVIOUR IN A NON-LINEAR ENVIRONMENT—ANALYSIS

We now examine the stochastic behaviour of the MOV-FXLMS algorithm (8) when applied to the non-linear environment depicted in Figure 1, with the saturation non-linearity given by (3).

In the non-linear system, the error expression becomes

$$e(n) = \mathbf{W}^0 \mathbf{X}(n) + z(n) - g[y_s(n)] \quad (11)$$

Taking initially the expected value of (8) conditioned on the set  $\mathcal{W} = \{\mathbf{W}(n), \mathbf{W}(n-1), \dots, \mathbf{W}(n-M+1)\}$  of the last  $M$  weight vectors yields

$$E\{\mathbf{W}(n+1)|\mathcal{W}\} = \mathbf{W}(n) + \mu E\{e(n)\mathbf{X}_f(n)|\mathcal{W}\} - \mu\gamma E\{\hat{y}_s(n)\mathbf{X}_f(n)|\mathcal{W}\} \quad (12)$$

Substituting (5), (9)–(11) in (12), and assuming  $M \geq \hat{M}$ ,<sup>||</sup> yields

$$\begin{aligned} E\{\mathbf{W}(n+1)|\mathcal{W}\} &= \mathbf{W}(n) + \mu \sum_{j=0}^{\hat{M}-1} \hat{s}_j E\{\mathbf{X}(n-j)\mathbf{X}^T(n)|\mathcal{W}\} \mathbf{W}^0 \\ &+ \mu \sum_{j=0}^{\hat{M}-1} \hat{s}_j E\{z(n)\mathbf{X}(n-j)|\mathcal{W}\} \\ &- \mu \sum_{j=0}^{\hat{M}-1} \hat{s}_j E\left\{g\left[\sum_{i=0}^{M-1} s_i \mathbf{W}^T(n-i)\mathbf{X}(n-i)\right]\mathbf{X}(n-j)|\mathcal{W}\right\} \\ &- \mu\gamma \sum_{i=0}^{\hat{M}-1} \sum_{j=0}^{\hat{M}-1} \hat{s}_i \hat{s}_j E\{\mathbf{X}(n-j)\mathbf{X}^T(n-i)|\mathcal{W}\} \mathbf{W}(n-i) \end{aligned} \quad (13)$$

Equation (13) clearly shows that the statistical analysis of the algorithm behaviour involves moments of products of the present and past values of data and weight vectors. Since the joint probability density function of the weights and data is not known, statistical approximations must be made to proceed with the analysis. The following assumptions are used for sufficiently small  $\mu$ :

A1:

$$E\{\mathbf{X}(n-j)\mathbf{X}^T(n)|\mathcal{W}\} \approx \mathbf{R}_{-j}, \quad 0 \leq j \leq M-1$$

A2:

$$E\{\mathbf{X}(n-j)\mathbf{X}^T(n-i)|\mathcal{W}\} \approx \mathbf{R}_{i-j}, \quad 0 \leq i, j \leq M-1$$

where  $\mathbf{R}_{k-\ell} = E\{\mathbf{X}(n-\ell)\mathbf{X}^T(n-k)\}$  is the correlation matrix of time-lagged input vectors.

A sufficient condition for these assumptions to hold is that weight and data vectors are statistically independent. Clearly, this is not true. In fact, A1 and A2 only imply that the statistical dependence of weight and data vectors is not significant in determining the algorithm behaviour. Similar assumptions have been made in Reference [5] and extensively verified by numerical simulations.

The third expectation in (13) is of the form  $E\{g(y_1)\mathbf{Y}_2\}$  where  $y_1 = \sum_{i=0}^{M-1} s_i \mathbf{W}^T(n-i)\mathbf{X}(n-i)$  and  $\mathbf{Y}_2 = \mathbf{X}(n-j)$ . This expectation can be evaluated using the procedure used to derive

<sup>||</sup>This is a reasonable assumption for practical implementations, where the estimated response is seldom longer than the actual secondary path response.

Reference [5, Equation (13)], leading to

$$E \left\{ g \left[ \sum_{i=0}^{M-1} s_i \mathbf{W}^T(n-i) \mathbf{X}(n-i) \right] \mathbf{X}(n-j) | \mathcal{H}^c \right\} \\ = \frac{\sum_{i=0}^{M-1} s_i \mathbf{R}_{i-j} \mathbf{W}(n-i)}{\left[ \frac{1}{\sigma^2} \sum_{j=0}^{M-1} \sum_{i=0}^{M-1} s_i s_j \mathbf{W}^T(n-j) \mathbf{R}_{i-j} \mathbf{W}(n-i) + 1 \right]^{1/2}} \quad (14)$$

Using A1, A2 and (14) in (13) and noting that  $E\{z(n)X(n-j)|\mathcal{H}^c\} = \mathbf{0}$  because  $z(n)$  is zero-mean and statistically independent of  $x(n)$ , yields

$$E\{\mathbf{W}(n+1)|\mathcal{H}^c\} = \mathbf{W}(n) + \mu \sum_{j=0}^{\hat{M}-1} \hat{s}_j \mathbf{R}_{-j} \mathbf{W}^0 - \mu \gamma \sum_{i=0}^{\hat{M}-1} \sum_{j=0}^{\hat{M}-1} \hat{s}_i \hat{s}_j \mathbf{R}_{i-j} \mathbf{W}(n-i) \\ - \mu \frac{\sum_{j=0}^{\hat{M}-1} \sum_{i=0}^{M-1} \hat{s}_j s_i \mathbf{R}_{i-j} \mathbf{W}(n-i)}{\left[ \frac{1}{\sigma^2} \sum_{j=0}^{M-1} \sum_{i=0}^{M-1} s_i s_j \mathbf{W}^T(n-j) \mathbf{R}_{i-j} \mathbf{W}(n-i) + 1 \right]^{1/2}} \quad (15)$$

The expected value of (15) can only be approximated since the joint probability density function of  $\mathbf{W}(n)$  and  $\mathbf{W}(m)$  is not known. A good approximation is obtained by noticing that  $\sum_{k=0}^{N-1} w_k(n-j)w_k(n-i)$  can be assumed weakly correlated with  $w_\ell(n-i)$  for large values of  $N$  and for all  $i, j$  and  $\ell$ . For ergodic signals, this is equivalent to apply the averaging principle proposed in Reference [20], as the value of the summation tends to be slowly varying when compared with  $w_\ell(n-i)$  for large  $N$ . Approximating  $\mathbf{W}(n)$  and  $\mathbf{W}^T(n-j)\mathbf{R}_{i-j}\mathbf{W}(n-i)$  by their expected values separately in the numerator and denominator of (15)\*\* and using

$$E\{\mathbf{W}^T(n-j)\mathbf{R}_{i-j}\mathbf{W}(n-i)\} = \text{tr}[\mathbf{R}_{i-j}E\{\mathbf{W}(n-i)\mathbf{W}^T(n-j)\}] \quad (16)$$

where  $\text{tr}[\cdot]$  is the trace of the matrix, leads to

$$E\{\mathbf{W}(n+1)\} = E\{\mathbf{W}(n)\} + \mu \sum_{j=0}^{\hat{M}-1} \hat{s}_j \mathbf{R}_{-j} \mathbf{W}^0 - \mu \gamma \sum_{i=0}^{\hat{M}-1} \sum_{j=0}^{\hat{M}-1} \hat{s}_i \hat{s}_j \mathbf{R}_{i-j} E\{\mathbf{W}(n-i)\} \\ - \mu \frac{\sum_{j=0}^{\hat{M}-1} \sum_{i=0}^{M-1} \hat{s}_j s_i \mathbf{R}_{i-j} E\{\mathbf{W}(n-i)\}}{\left[ \frac{1}{\sigma^2} \sum_{j=0}^{M-1} \sum_{i=0}^{M-1} s_i s_j \text{tr}\{\mathbf{R}_{i-j}\mathbf{K}_{i,j}(n)\} + 1 \right]^{1/2}} \quad (17)$$

where

$$\mathbf{K}_{i,j}(n) = E\{\mathbf{W}(n-i)\mathbf{W}^T(n-j)\} \quad (18)$$

is the cross-correlation matrix of delayed weight vectors. Note that for  $\gamma = 0$  (17) reduces to the mean weight equation for the FXLMS with non-linear secondary path derived in Reference [5]. For sufficiently small  $\mu$ ,  $\mathbf{K}_{i,j}(n)$  can be approximated as

$$\mathbf{K}_{i,j}(n) \approx E\{\mathbf{W}(n-i)\}E\{\mathbf{W}^T(n-j)\} \quad (19)$$

which completes the model for the mean weight behaviour.

\*\*This approximation has been successfully applied in References [4,5].

## 5. THE OPTIMAL PENALTY FACTOR

In this section, we show that the MOV-FXLS algorithm leads to a biased steady-state mean weight solution. Then, we determine how the effort penalty factor  $\gamma$  in (4) can be designed to control the steady-state bias.

## 5.1. Mean steady-state weight vector

Assuming convergence as  $n \rightarrow \infty$ , defining  $\mathbf{W}_\infty = \lim_{n \rightarrow \infty} E\{\mathbf{W}(n)\}$ , using (19) in (17) and solving it for  $\mathbf{W}_\infty$  yields

$$\mathbf{W}_\infty = \left[ \gamma \tilde{\mathbf{R}}_{\hat{\mathbf{S}}\hat{\mathbf{S}}} + \frac{1}{\left(\frac{1}{\sigma^2} \mathbf{W}_\infty^T \tilde{\mathbf{R}}_{\mathbf{S}\mathbf{S}} \mathbf{W}_\infty + 1\right)^{1/2}} \tilde{\mathbf{R}}_{\hat{\mathbf{S}}\mathbf{S}} \right]^{-1} \tilde{\mathbf{R}}_{\hat{\mathbf{S}}\mathbf{S}} \mathbf{W}^0 \quad (20)$$

where

$$\begin{aligned} \tilde{\mathbf{R}}_{\hat{\mathbf{S}}\mathbf{S}} &= \sum_{j=0}^{\hat{M}-1} \sum_{i=0}^{M-1} \hat{s}_j s_i \mathbf{R}_{i-j} \\ \tilde{\mathbf{R}}_{\hat{\mathbf{S}}} &= \sum_{j=0}^{\hat{M}-1} \hat{s}_j \mathbf{R}_{-j} \\ \tilde{\mathbf{R}}_{\mathbf{S}\mathbf{S}} &= \sum_{j=0}^{M-1} \sum_{i=0}^{M-1} s_i s_j \mathbf{R}_{i-j} \\ \tilde{\mathbf{R}}_{\hat{\mathbf{S}}\hat{\mathbf{S}}} &= \sum_{j=0}^{\hat{M}-1} \sum_{i=0}^{\hat{M}-1} \hat{s}_i \hat{s}_j \mathbf{R}_{i-j} \end{aligned} \quad (21)$$

Up to this point, the results are valid for any  $\mathbf{S}$  and  $\hat{\mathbf{S}}$ . To proceed with the determination of the optimum penalty factor, we assume from now on that  $\hat{\mathbf{S}}$  is a good estimate of  $\mathbf{S}$ , or  $\hat{\mathbf{S}} \approx \mathbf{S}$ . In this case (20) reduces to

$$\mathbf{W}_\infty = v \tilde{\mathbf{R}}_{\mathbf{S}\mathbf{S}}^{-1} \tilde{\mathbf{R}}_{\mathbf{S}} \mathbf{W}^0 \quad (22)$$

where

$$v = \frac{1}{\gamma + \frac{1}{\left(\frac{1}{\sigma^2} \mathbf{W}_\infty^T \tilde{\mathbf{R}}_{\mathbf{S}\mathbf{S}} \mathbf{W}_\infty + 1\right)^{1/2}}} \quad (23)$$

and

$$\tilde{\mathbf{R}}_{\mathbf{S}} = \sum_{j=0}^{M-1} s_j \mathbf{R}_{-j} \quad (24)$$

Using (22) in (23) yields

$$v = \frac{1}{\gamma + \frac{1}{(v^2 \beta^2 + 1)^{1/2}}} \quad (25)$$

where

$$\beta^2 = \frac{1}{\sigma^2} \mathbf{W}^0 \mathbf{T} \tilde{\mathbf{R}}_S \tilde{\mathbf{R}}_{SS}^{-1} \tilde{\mathbf{R}}_S \mathbf{W}^0 \quad (26)$$

Note that  $v$  is a positive scalar since  $\gamma$ ,  $\beta^2$  and  $v^2$  are positive. More importantly, note that the steady-state weight scale factor  $v$  is a function of the penalty factor  $\gamma$ , which is a design parameter. The degree of non-linearity  $\beta^2$  is defined as the ratio of the average steady-state power of the cancelling signal  $y_g(n)$  in the linear case (equal to  $y_s(n)$ ) to the maximum non-linear output power ( $\lim_{y_s \rightarrow \infty} g(y_s)$ ) [5, Equation (30)]. In the particular case studied here  $\hat{\mathbf{S}} = \mathbf{S}$ .

### 5.2. Optimum penalty factor

It was shown in Reference [17, Equation (15)] that the weight vector at the minimum of the performance surface corresponding to the non-linear estimation problem in Figure 1 is given by

$$\tilde{\mathbf{W}} = \sqrt{1 - \frac{1}{2\beta^2} + \sqrt{1 + \frac{1}{4\beta^4}}} \times \tilde{\mathbf{R}}_{SS}^{-1} \tilde{\mathbf{R}}_S \mathbf{W}^0 = \alpha \tilde{\mathbf{R}}_{SS}^{-1} \tilde{\mathbf{R}}_S \mathbf{W}^0 \quad (27)$$

Comparing (27) and (22) shows that the MOV-FXLMS algorithm leads to a steady-state solution that is collinear with the optimal solution for  $\hat{\mathbf{S}} = \mathbf{S}$ . Thus, an unbiased steady-state solution can be obtained by making  $v = \alpha$ .<sup>††</sup>

Solving (23) for  $\gamma$  leads to the solution

$$\gamma = \frac{1}{v} - \frac{1}{\sqrt{v^2 \beta^2 + 1}} \quad (28)$$

which for

$$v = \alpha = \sqrt{1 - \frac{1}{2\beta^2} + \sqrt{1 + \frac{1}{4\beta^4}}} \quad (29)$$

leads to the expression for the optimum value of  $\gamma$ :

$$\gamma_{\text{opt}} = \frac{1}{v} - \frac{1}{\sqrt{v^2 \beta^2 + 1}} = \frac{1}{\sqrt{1 - \frac{1}{2\beta^2} + \sqrt{1 + \frac{1}{4\beta^4}}}} - \frac{1}{\sqrt{\frac{1}{2} + \beta^2 + \sqrt{\frac{1}{4} + \beta^4}}} \quad (30)$$

which is the effort penalty factor that leads to an unbiased steady-state solution. Figure 2 shows the variation of  $\gamma_{\text{opt}}$  as a function of the degree of non-linearity  $\beta^2$ . Note that  $\gamma_{\text{opt}} = 0$  for  $\beta^2 = 0$ . This shows that the optimally designed MOV-FXLMS algorithm ( $\gamma = \gamma_{\text{opt}}$ ) becomes the FXLMS algorithm in the linear case ( $\beta = 0$ ).

### 5.3. Design issues

Though (30) gives the design value of  $\gamma_{\text{opt}}$ , this expression is a function of parameter  $\beta^2$ , which must be estimated in practical applications. An estimate of  $\beta^2$  can be obtained from the steady-

<sup>††</sup>Note that (22) corresponds to the minimum MSE solution (27) multiplied by a non-unity scalar factor if  $v \neq \alpha$ . This non-unity scalar factor constitutes a multiplicative bias to the optimum solution. An unbiased solution is obtained for  $v = \alpha$  in (22), with  $\alpha$  defined in (27).

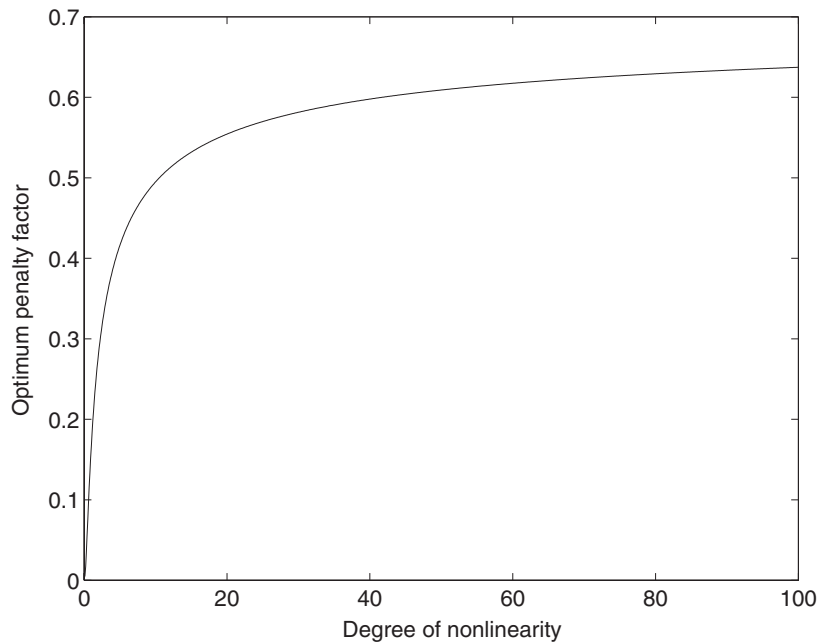


Figure 2. Optimum penalty factor  $\gamma_{\text{opt}}$  as a function of the degree of non-linearity  $\beta^2$ .

state behaviour of the FXLMS algorithm, which corresponds to the MOV-FXLMS algorithm for  $\gamma = 0$ . It is easy to show from (25) that for  $\gamma = 0$ , and assuming  $\hat{\mathbf{S}} = \mathbf{S}$ ,

$$v = \frac{1}{\sqrt{1 - \beta^2}} \quad (31)$$

with  $\beta^2$  given by (26). Also, from (5) and assuming convergence,

$$\lim_{n \rightarrow \infty} y_s(n) = \sum_{i=0}^{M-1} s_i \mathbf{W}_{\infty}^T \mathbf{X}(n-i) \quad (32)$$

and then

$$E\{y_s^2(n)\}_{n \rightarrow \infty} = \mathbf{W}_{\infty}^T \tilde{\mathbf{R}}_{\text{SS}} \mathbf{W}_{\infty} \quad (33)$$

Now, using (22) and (31) in (33) and recognizing from (26) that  $\mathbf{W}^0 \mathbf{R}_{\text{S}}^T \tilde{\mathbf{R}}_{\text{SS}}^{-1} \tilde{\mathbf{R}}_{\text{S}} \mathbf{W}^0 = \sigma^2 \beta^2$  yields

$$E\{y_s^2(n)\}_{n \rightarrow \infty} = \frac{\sigma^2 \beta^2}{1 - \beta^2} \quad (34)$$

and thus

$$\beta^2 = \frac{E\{y_s^2(n)\}_{n \rightarrow \infty}}{E\{y_s^2(n)\}_{n \rightarrow \infty} + \sigma^2} \quad (35)$$

An estimate of  $\sigma^2$  can be obtained by noting that [5]

$$\max\{y_g^2(n)\} = \frac{\pi}{2} \sigma^2 = \lim_{y \rightarrow \infty} g(y) \quad (36)$$

Thus,

$$\sigma^2 = \frac{2}{\pi} \max\{y_g^2(n)\} \quad (37)$$

which can be estimated off-line by driving the non-linearity into saturation and measuring its output.

An estimate of  $E\{y_s^2(n)\}|_{n \rightarrow \infty}$  can be obtained as the average steady-state power of the cancelling signal in the linear case ( $g(y_s) = y_s$ ) with  $\gamma = 0$ . To this end, an estimate  $\hat{\mathbf{S}}$  of  $\mathbf{S}$  must be obtained off-line. This can be accomplished using a low power excitation so that the actuator (speaker in ANC systems) is not driven into saturation. Then, the system in Figure 1 can be implemented with the sub-system composed by  $\mathbf{S}$  and  $g(y_s)$  replaced by  $\hat{\mathbf{S}}$ , using  $\gamma = 0$ , and with the cancellation point implemented within the signal processor. The output of the replacement  $\hat{\mathbf{S}}$  can then be used as an estimate  $\hat{y}_s(n)$  for  $y_s(n)$ .

The estimation of  $\beta^2$  using the technique described above assumes that the non-linearity model given by (3) is accurate. It will be shown in the next section that the performance of the MOV-FXLMS algorithm is robust to errors in this estimation for moderate and large degrees of non-linearity.

## 6. MEAN SQUARE ERROR BEHAVIOUR

The expression for the MSE conditioned on  $\mathcal{W}$  has been derived in Reference [5] using A1, A2 and is given by

$$\begin{aligned} E\{e^2(n)|\mathcal{W}\} &= \sigma_z^2 + \mathbf{W}^0 \mathbf{T} \mathbf{R}_0 \mathbf{W}^0 - \frac{2 \sum_{i=0}^{M-1} s_i \mathbf{W}^0 \mathbf{T} \mathbf{R}_i \mathbf{W}(n-i)}{\sqrt{\frac{1}{\sigma^2} \sum_{j=0}^{M-1} \sum_{i=0}^{M-1} s_j s_i \mathbf{W}^T(n-j) \mathbf{R}_{i-j} \mathbf{W}(n-i) + 1}} \\ &+ \sigma^2 \sin^{-1} \left( \frac{\sum_{j=0}^{M-1} \sum_{i=0}^{M-1} s_j s_i \mathbf{W}^T(n-j) \mathbf{R}_{i-j} \mathbf{W}(n-i)}{\sum_{j=0}^{M-1} \sum_{i=0}^{M-1} s_j s_i \mathbf{W}^T(n-j) \mathbf{R}_{i-j} \mathbf{W}(n-i) + \sigma^2} \right) \end{aligned} \quad (38)$$

where  $\mathbf{R}_0 = E\{\mathbf{X}(n)\mathbf{X}^T(n)\}$  is the input vector autocorrelation matrix.

Using the same approximations used to derive (17) and (19) from (15) leads to an expression for the MSE for sufficiently small  $\mu$ :

$$\begin{aligned} \xi(n) = E\{e^2(n)\} &\approx \sigma_z^2 + \mathbf{W}^0 \mathbf{T} \mathbf{R}_0 \mathbf{W}^0 \\ &- \frac{2 \sum_{i=0}^{M-1} s_i \mathbf{W}^0 \mathbf{T} \mathbf{R}_i E\{\mathbf{W}(n-i)\}}{\sqrt{\frac{1}{\sigma^2} \sum_{j=0}^{M-1} \sum_{i=0}^{M-1} s_j s_i E\{\mathbf{W}^T(n-j)\} \mathbf{R}_{i-j} E\{\mathbf{W}(n-i)\} + 1}} \\ &+ \sigma^2 \sin^{-1} \left( \frac{\sum_{j=0}^{M-1} \sum_{i=0}^{M-1} s_j s_i E\{\mathbf{W}^T(n-j)\} \mathbf{R}_{i-j} E\{\mathbf{W}(n-i)\}}{\sum_{j=0}^{M-1} \sum_{i=0}^{M-1} s_j s_i E\{\mathbf{W}^T(n-j)\} \mathbf{R}_{i-j} E\{\mathbf{W}(n-i)\} + \sigma^2} \right) \end{aligned} \quad (39)$$

where the mean weight vectors are determined using (17), which includes the dependence on the effort penalty factor  $\gamma$ .

### 6.1. Steady-state mean square error

Substituting  $\mathbf{W}_\infty$  for  $E\{\mathbf{W}(n-i)\}$  and  $E\{\mathbf{W}(n-j)\}$  in (39), using (22) and (23) with  $\gamma = \gamma_{\text{opt}}$  given by (30) yields the steady-state MSE for the optimally designed MOV-FXLMS algorithm:

$$\lim_{n \rightarrow \infty} \xi(n) = \sigma_z^2 + \mathbf{W}^{\text{oT}} \mathbf{R}_0 \mathbf{W}^{\text{o}} + \mathbf{W}^{\text{oT}} \tilde{\mathbf{R}}_S^{\text{T}} \tilde{\mathbf{R}}_{SS}^{-1} \tilde{\mathbf{R}}_S \mathbf{W}^{\text{o}} \left[ \frac{1}{\beta^2} \sin^{-1} \left( \frac{v^2 \beta^2}{v^2 \beta^2 + 1} \right) - \frac{2v}{\sqrt{v^2 \beta^2 + 1}} \right] \quad (40)$$

where  $v$  can be obtained from the solution of (25). Note that (40) agrees with the expression for the minimum of the MSE surface derived in Reference [17] for the non-linear mean square estimation associated with the system in Figure 1.

## 7. SIMULATION RESULTS

This section presents simulation results in support of the theoretical models and to verify the applicability of the MOV-FXLMS algorithm. Representative plots have been selected from a large number of results. The optimal penalty factor  $\gamma$  calculated from (30) has been used for all examples, with  $\beta^2$  evaluated using (26). In the examples where  $\hat{\mathbf{S}} \neq \mathbf{S}$ , the degree of non-linearity  $\beta^2$  evaluated from (26) leads to a value of  $\gamma$  obtained from (30) that is not optimal, since  $\gamma_{\text{opt}}$  has been determined for  $\hat{\mathbf{S}} = \mathbf{S}$ . These examples were chosen to illustrate the robustness of the algorithm to errors in the estimate of the degree of non-linearity  $\beta^2$ .

### 7.1. Example 1

Consider  $\mathbf{W}^{\text{o}} = [0.4130 \ 0.4627 \ 0.4803 \ 0.4627 \ 0.4130]^{\text{T}}$ ,  $\mathbf{W}^{\text{oT}} \mathbf{W}^{\text{o}} = 1$ ,  $x(n)$  white with variance  $\sigma_x^2 = 1$ , measurement noise  $z(n)$  with  $\sigma_z^2 = 10^{-6}$  and perfect secondary path estimation with  $\hat{\mathbf{S}} = \mathbf{S} = [0.9325 \ 0.2798 \ 0.1865 \ 0.0933 \ 0.0933]^{\text{T}}$ . Simulations are presented for three step sizes (normalized with respect to the linear FXLMS stability limit). The stability limit  $\mu_{\text{max}} \approx 0.2$  has been determined by simulation. Step sizes  $\mu_1 = \mu_{\text{max}}/5$ ,  $\mu_2 = \mu_{\text{max}}/10$  and  $\mu_3 = \mu_{\text{max}}/100$  have been used to evaluate the models for large, moderate and small  $\mu$ . Also,  $\beta^2 = 0.0001, 0.3, 0.5$  and  $0.9$  have been selected to illustrate the model accuracy for small, moderate and large degrees of non-linearity. Figures 3(a), (c) and (e) compare the simulated mean weight behaviour with the analytical predictions using (17). Each plot presents the results for  $\beta^2 = 0.0001, 0.3$  and  $0.9$  and a single  $\mu$ , averaged over 1000 realizations. Three vector components were selected at random to conserve space. The remaining components have similar behaviour. The analytical model is accurate even for relatively large step sizes.

Figures 3(b), (d) and (f) show the simulated MSE and the theoretical MSE using (39). Each figure shows curves for  $\beta^2 = 0.0001, 0.3, 0.5$  and  $0.9$ . Plots are shown for different step sizes. All plots were obtained by averaging 1000 runs. The analytical model and the simulations are in close agreement in all cases, even for the relatively large  $\mu = \mu_1$ . The analysis of these plots show that, in general, the steady-state MSE decreases with the step size  $\mu$ . This decrease, however, becomes less significant as the degree of non-linearity increases (see, for instance, the curves labeled IV). Such behaviour is expected because a large degree of non-linearity (strong

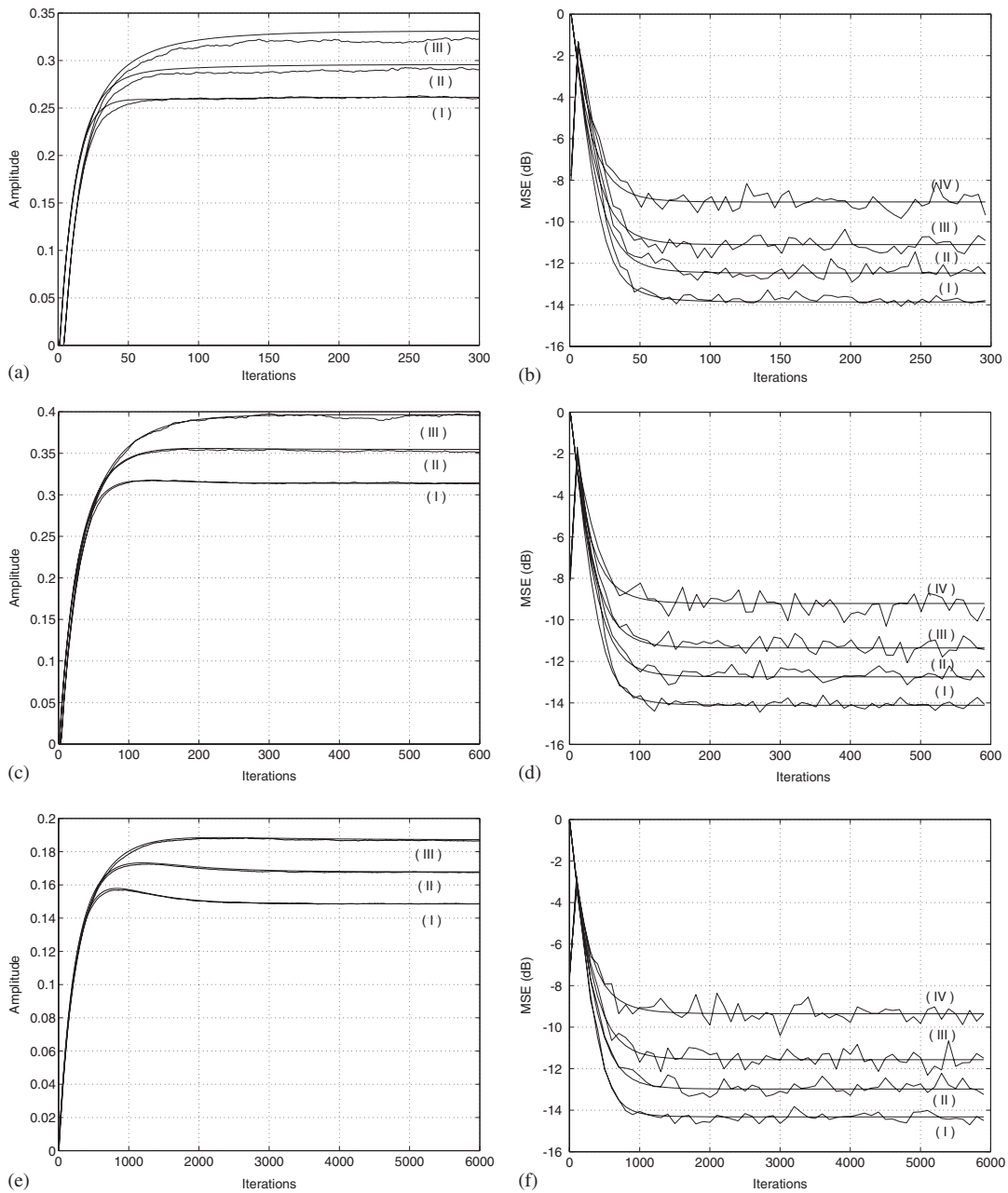


Figure 3. Example 1: left column:  $E\{\mathbf{W}(n)\}$  for  $\beta^2 = 0.0001$  (curve (I)), 0.3 (curve (II)) and 0.9 (curve (III)). Plots (a), (c) and (e) for different values of  $\mu$ . Right column: MSE in dB for  $\beta^2 = 0.0001$  (curve (I)), 0.3 (curve (II)), 0.5 (curve (III)) and 0.9 (curve (IV)). Plots (b), (d) and (f) for different values of  $\mu$ . All plots averaged over 1000 runs. Simulation—ragged curves. Theory—smooth curves.  $\gamma = \gamma_{opt}$  in all cases: (a)  $E\{w_4(n)\}$  for  $\mu_1 = \frac{\mu_{max}}{5} = 0.04$ ; (b) MSE (dB) for  $\mu_1 = \frac{\mu_{max}}{5} = 0.04$ ; (c)  $E\{w_3(n)\}$  for  $\mu_2 = \frac{\mu_{max}}{10} = 0.02$ ; (d) MSE (dB) for  $\mu_2 = \frac{\mu_{max}}{10} = 0.02$ ; (e)  $E\{w_5(n)\}$  for  $\mu_3 = \frac{\mu_{max}}{100} = 0.002$  and (f) MSE (dB) for  $\mu_3 = \frac{\mu_{max}}{100} = 0.002$ .

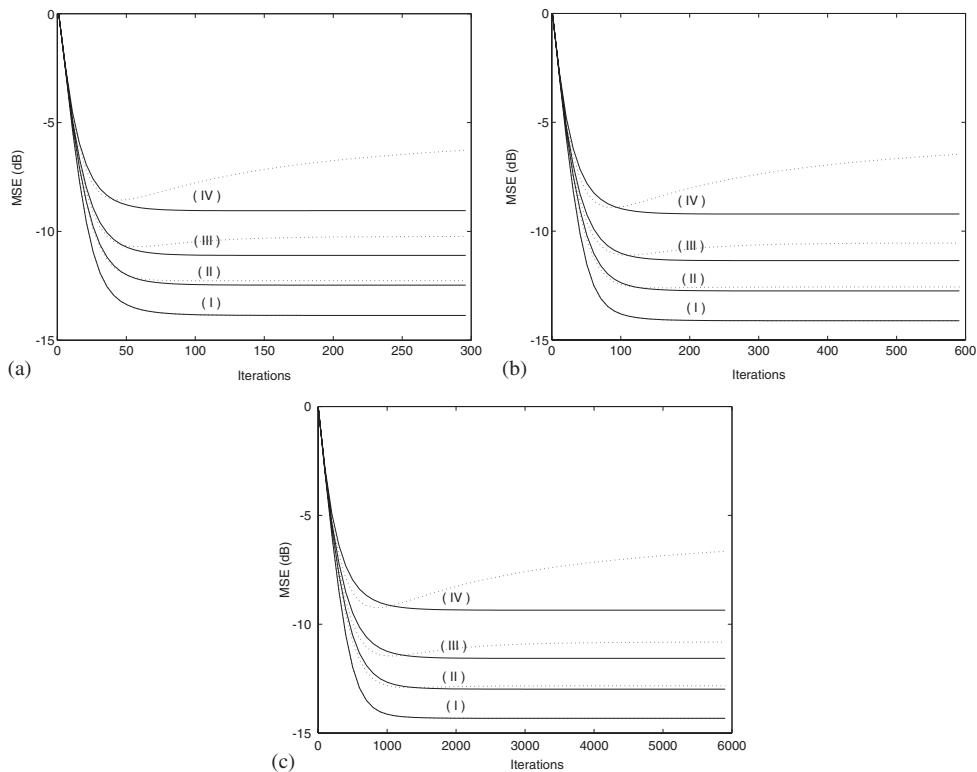


Figure 4. Example 1: comparison between MOV-FXLMS and FXLMS algorithms. MSE in dB for  $\beta^2 = 0.0001$  (curve (I)), 0.3 (curve (II)), 0.5 (curve (III)) and 0.9 (curve (IV)). Plots (a)–(c) for different values of  $\mu$ . Curves drawn using the analytical models derived in this work (MOV-FXLMS) and in Reference [5] (FXLMS). FXLMS: dotted line. MOV-FXLMS: continuous line: (a) MSE (dB) for  $\mu_1 = \frac{\mu_{\max}}{5} = 0.04$ ; (b) MSE (dB) for  $\mu_2 = \frac{\mu_{\max}}{10} = 0.02$  and (c) MSE (dB) for  $\mu_3 = \frac{\mu_{\max}}{100} = 0.002$ .

saturation) limits the ability of the adaptive filter to cancel the desired signal  $d(n)$ . For large values of  $\beta$ ,  $y_g(n)$  cannot follow the variations of  $y_s(n)$  dictated by the adaptive filter.

Figures 4(a)–(c) compare the performances of the MOV-FXLMS and FXLMS ( $\gamma = 0$ ) algorithms. Note that the MOV-FXLMS algorithm performs significantly better than the FXLMS algorithm for moderate and large degrees of non-linearity.

## 7.2. Example 2

This example repeats Example 1 for a longer impulse response  $\mathbf{W}^0$  and for an imperfect estimate of the secondary path. Consider  $\mathbf{W}^0 = [0.0156 \ 0.0598 \ 0.1260 \ 0.2041 \ 0.2822 \ 0.3485 \ 0.3927 \ 0.4083 \ 0.3927 \ 0.3485 \ 0.2822 \ 0.2041 \ 0.1260 \ 0.0598 \ 0.0156]^T$ ,  $\mathbf{W}^{0T}\mathbf{W}^0 = 1$ ,  $\mathbf{S} = [0.9356 \ 0.2807 \ 0.1871 \ 0.0936 \ 0.0468]^T$ ,  $\mathbf{S}^T\mathbf{S} = 1$ ,  $\hat{\mathbf{S}} = [0.8922 \ 0.3965 \ 0.1487 \ 0.1487 \ 0.0496]^T$ ,  $\hat{\mathbf{S}}^T\hat{\mathbf{S}} = 1$ ,  $x(n)$  white with  $\sigma_x^2 = 1$  and  $\sigma_z^2 = 10^{-6}$ . The stability limit  $\mu_{\max} = 0.05$  was determined by simulation. The parameters were  $\mu_1 = \mu_{\max}/5$ ,  $\mu_2 = \mu_{\max}/10$ ,  $\mu_3 = \mu_{\max}/100$  and  $\beta^2 = 0.0001$ , 0.3, 0.5 and 0.9.

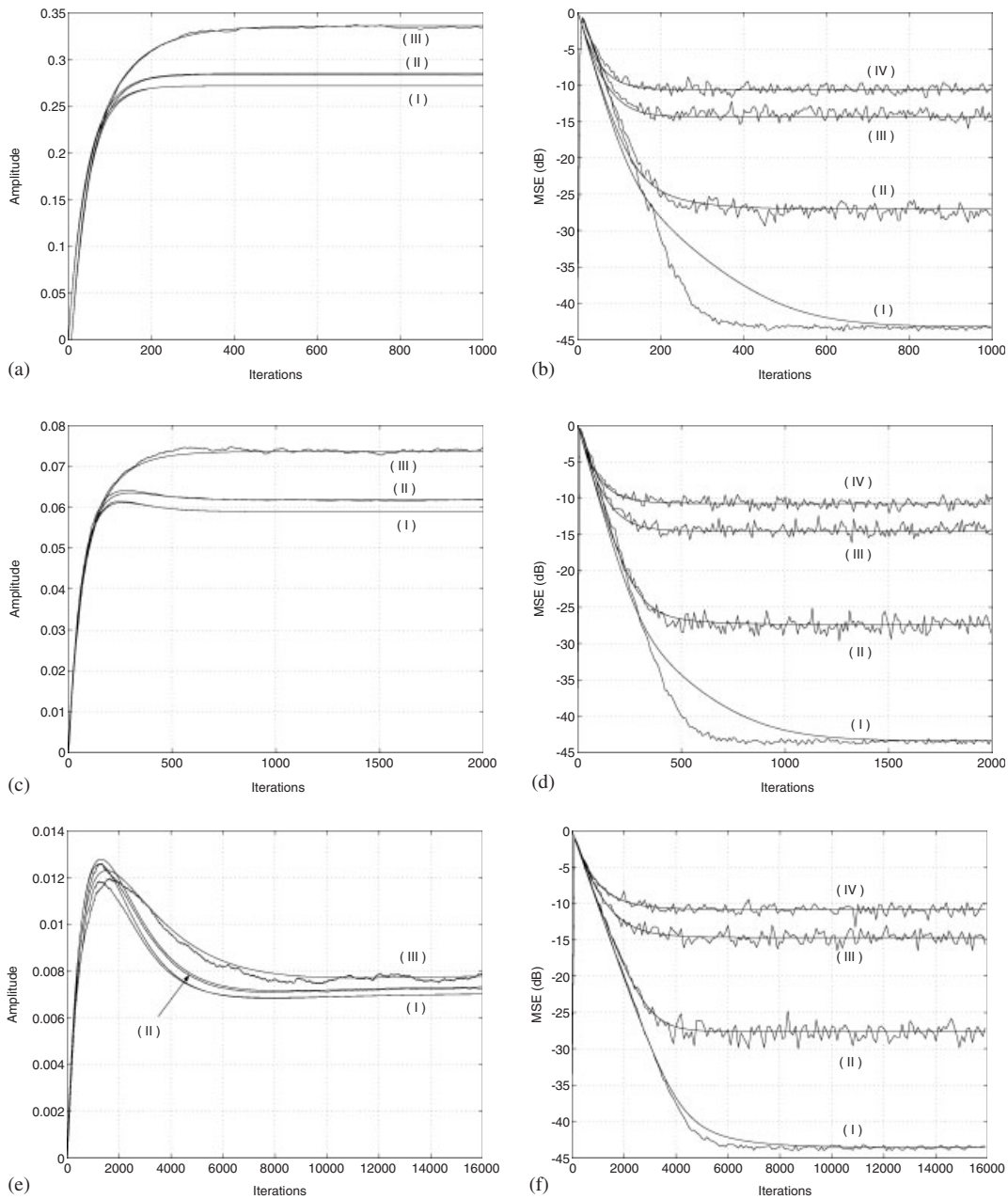


Figure 5. Example 2: left column:  $E\{\mathbf{W}(n)\}$  for  $\beta^2 = 0.0001$  (curve (I)), 0.3 (curve (II)) and 0.9 (curve (III)). Plots (a), (c) and (e) for different values of  $\mu$ . Right column: MSE in dB for  $\beta^2 = 0.0001$  (curve (I)), 0.3 (curve (II)), 0.5 (curve (III)) and 0.9 (curve (IV)). Plots (b), (d) and (f) for different values of  $\mu$ . All plots averaged over 1000 runs. Simulation—ragged curves. Theory—smooth curves.  $\gamma$  determined from (30) in all cases: (a)  $E\{w_8(n)\}$  for  $\mu_1 = \frac{\mu_{\max}}{5} = 0.01$ ; (b) MSE (dB) for  $\mu_1 = \frac{\mu_{\max}}{5} = 0.01$ ; (c)  $E\{w_2(n)\}$  for  $\mu_2 = \frac{\mu_{\max}}{10} = 0.005$ ; (d) MSE (dB) for  $\mu_2 = \frac{\mu_{\max}}{10} = 0.005$ ; (e)  $E\{w_4(n)\}$  for  $\mu_3 = \frac{\mu_{\max}}{100} = 0.0005$  and (f) MSE (dB) for  $\mu_3 = \frac{\mu_{\max}}{100} = 0.0005$ .

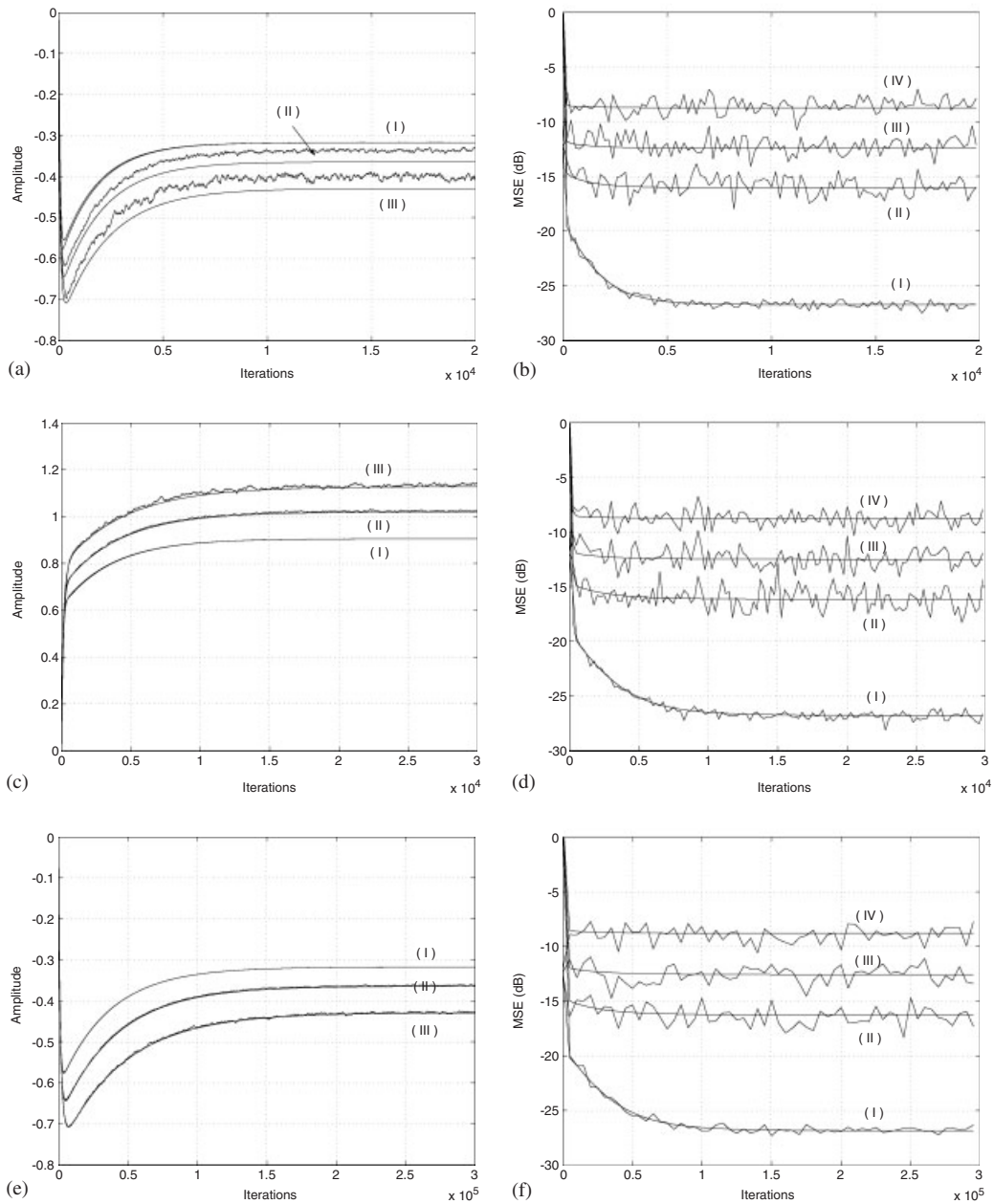


Figure 6. Example 3: left column:  $E\{\mathbf{W}(n)\}$  for  $\beta^2 = 0.0001$  (curve (I)), 0.3 (curve (II)) and 0.9 (curve (III)). Plots (a), (c) and (e) for different values of  $\mu$ . Right column: MSE in dB for  $\beta^2 = 0.0001$  (curve (I)), 0.3 (curve (II)), 0.5 (curve (III)) and 0.9 (curve (IV)). Plots (b), (d) and (f) for different values of  $\mu$ . All plots averaged over 1000 runs. Simulation—ragged curves. Theory—smooth curves.  $\gamma$  determined from (30) in all cases: (a)  $E\{w_3(n)\}$  for  $\mu_1 = \frac{\mu_{\max}}{5} = 0.012$ ; (b) MSE (dB) for  $\mu_1 = \frac{\mu_{\max}}{5} = 0.012$ ; (c)  $E\{w_1(n)\}$  for  $\mu_2 = \frac{\mu_{\max}}{10} = 0.006$ ; (d) MSE (dB) for  $\mu_2 = \frac{\mu_{\max}}{10} = 0.006$ ; (e)  $E\{w_4(n)\}$  for  $\mu_3 = \frac{\mu_{\max}}{100} = 0.0006$  and (f) MSE (dB) for  $\mu_3 = \frac{\mu_{\max}}{100} = 0.0006$ .

Figure 5 verifies the analytical model using recursions (17) and (39). Different weights were chosen for each step size, as compared to Example 1, in order to provide a broader assessment of the system behaviour. Figures 5(b) and (d) indicate that the model sometimes deviates from the simulation for large step sizes and small degrees of non-linearity. The mismatch is minimal for small  $\mu$  (Figure 5(f)), used in most practical applications (see, Reference [21] for instance). The model is accurate for the initial transient phase (cancellation to  $-30$  dB, compatible with most practical applications) and in steady state, even for large  $\mu$ .

### 7.3. Example 3

This example verifies the model accuracy for correlated inputs.  $x(n)$  is an autoregressive process with  $\sigma_x^2 = 1$ , obtained by passing a white noise  $u(n)$  with variance  $\sigma_u^2 = 0.0965$  through the filter with attenuation given by  $A(z) = 1 - 0.195z^{-1} + 0.95z^{-2}$ . The eigenvalue spread of  $\mathbf{R}_0$  is equal to 39.82 [22].  $\mathbf{W}^o = [0.7756 \ 0.5171 \ -0.3620]^T$ ,  $\mathbf{S} = [0.8944 \ 0.4472]^T$ ,  $\hat{\mathbf{S}} = [0.9701 \ 0.2425]^T$  (imperfect secondary path estimation).  $\mu_{\max} = 0.06$  (experimentally

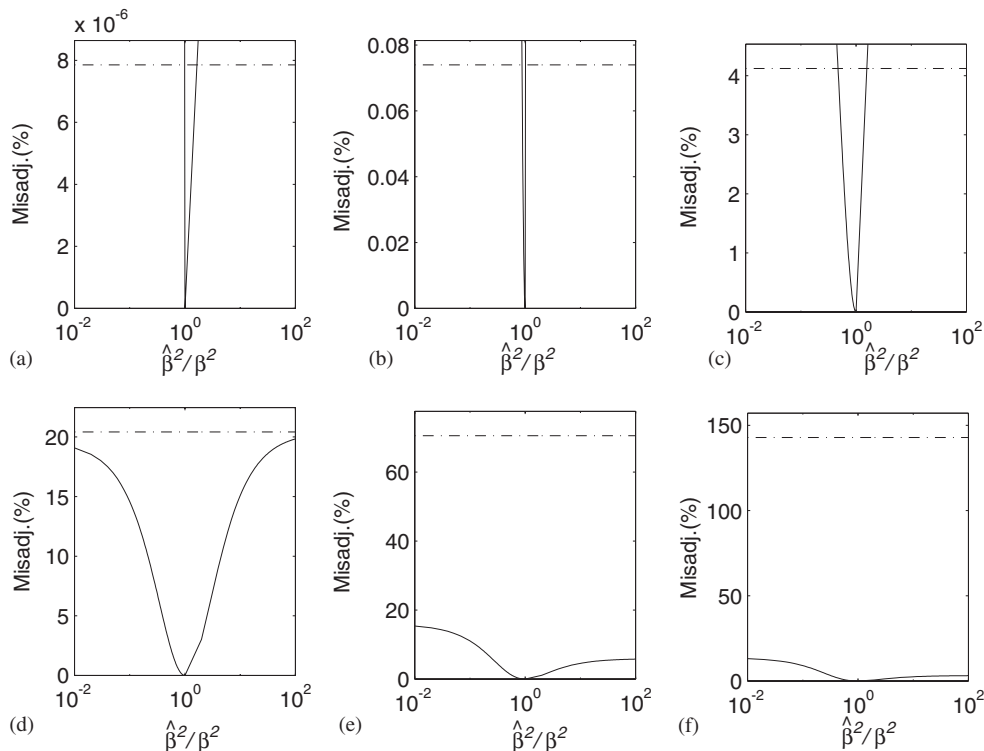


Figure 7. Comparisons between steady-state misadjustments (%) for the FXLMS and the MOV-FXLMS algorithm as a function of errors in estimating  $\gamma_{\text{opt}}$ : (a)  $\beta^2 = 0.01$ ; (b)  $\beta^2 = 0.1$ ; (c)  $\beta^2 = 0.3$ ; (d)  $\beta^2 = 0.5$ ; (e)  $\beta^2 = 0.7$  and (f)  $\beta^2 = 0.9$ . Vertical axes: misadjustment (%). Horizontal axes:  $\hat{\beta}^2/\beta^2$ , where  $\hat{\beta}^2$  is the estimated value of  $\beta^2$ . Horizontal lines: misadjustment for the FXLMS algorithm. Curved lines: misadjustment for the MOV-FXLMS algorithm.

obtained for the linear case). The parameters used were again  $\mu_1 = \mu_{\max}/5$ ,  $\mu_2 = \mu_{\max}/10$ ,  $\mu_3 = \mu_{\max}/100$  and  $\beta^2 = 0.0001, 0.3, 0.5$  and  $0.9$ . Figure 6 shows the theoretical and simulated results.

#### 7.4. Robustness to errors in parameter estimates

These results verify the robustness of the MOV-FXLMS algorithm to errors in parameter estimations and compare its steady-state performance with FXLMS. Consider  $\mathbf{W}^0 = [0.4130 \ 0.4627 \ 0.4803 \ 0.4627 \ 0.4130]^T$  and  $\hat{\mathbf{S}} = \mathbf{S} = [0.9325 \ 0.2798 \ 0.1865 \ 0.0933 \ 0.0933]^T$ . The input sequence is a zero-mean Gaussian, correlated signal with variance  $\sigma_x^2 = 1$  and with eigenvalue spread of its autocorrelation matrix equal to 10.34. The measurement noise is white Gaussian with variance  $\sigma_z^2 = 10^{-6}$ . Figure 7 compares the steady-state misadjustments achieved by the FXLMS algorithm (horizontal lines) and by the MOV-FXLMS algorithm (curved lines) as a function of the error in estimating  $\beta^2$ . Defining  $\hat{\beta}^2$  as the estimated value of  $\beta^2$ , the misadjustment is defined as

$$\mathcal{M} = \frac{\xi(\infty)|_{\beta^2} - \xi(\infty)|_{\hat{\beta}^2}}{\xi(\infty)|_{\beta^2}} \quad (41)$$

with  $\xi(\infty)$  defined by (40). Note that (41) refers only to the misadjustment due to an error in the estimation of  $\beta^2$ . This does not include the misadjustment due to weight fluctuations about the mean value, which are controlled by the step size  $\mu$ . Thus, a correct estimation  $\hat{\beta}^2 = \beta^2$  leads to  $\mathcal{M} = 0$ .

Each subplot is for a different degree of non-linearity  $\beta^2$  in  $\{0.01, 0.1, 0.3, 0.5, 0.7, 0.9\}$ . The vertical axes give the misadjustment and the horizontal axes the ratio  $\hat{\beta}^2/\beta^2$ , where  $\hat{\beta}^2$  stands for the estimated value of  $\beta^2$ . Figure 7 shows that the robustness of the MOV-FXLMS algorithm increases with the degree of non-linearity  $\beta^2$ . It can also be verified from Figure 7 that the MOV-FXLMS can perform much better than the FXLMS algorithm even for significant estimation errors for moderate and large degrees of non-linearity.

## 8. CONCLUSIONS

This paper has proposed a new adaptive algorithm to be used in ANC systems with a saturation non-linearity in the secondary path. The MOV-FXLMS algorithm belongs to the family of minimum effort algorithms, and implicitly controls the non-linear distortion by limiting the signal amplitude at the non-linearity input. Statistical analysis and simulation results show that the new algorithm outperforms the FXLMS algorithm, specially for moderate and large degrees of non-linearity. The optimal design of the new algorithm has been studied, with the determination of the optimal penalty factor that leads to an unbiased solution. The estimation of the necessary parameters for a practical design has been addressed. It has been verified that the MOV-FXLMS steady-state misadjustment improvement over the FXLMS performance is robust to errors in estimating the system's degree of non-linearity for moderate and large degrees of non-linearity.

## APPENDIX A: EVALUATION OF (8)

From (4),

$$\begin{aligned}
\sum_{j=0}^{M-1} \frac{\partial J(n)}{\partial \mathbf{W}(n-j)} &= \sum_{j=0}^{M-1} \frac{\partial [e^2(n) + \gamma y_s^2(n)]}{\partial \mathbf{W}(n-j)} \\
&= \sum_{j=0}^{M-1} \frac{\partial e^2(n)}{\partial \mathbf{W}(n-j)} + \gamma \sum_{j=0}^{M-1} \frac{\partial y_s^2(n)}{\partial \mathbf{W}(n-j)} \\
&= 2e(n) \sum_{j=0}^{M-1} \frac{\partial e(n)}{\partial \mathbf{W}(n-j)} + 2\gamma y_s(n) \sum_{j=0}^{M-1} \frac{\partial y_s(n)}{\partial \mathbf{W}(n-j)} \tag{A1}
\end{aligned}$$

Using (5) and (6) yields

$$\begin{aligned}
\sum_{j=0}^{M-1} \frac{\partial J(n)}{\partial \mathbf{W}(n-j)} &= 2e(n) \sum_{j=0}^{M-1} \frac{\partial}{\partial \mathbf{W}(n-j)} \left[ \mathbf{W}^0 \mathbf{X}(n) + z(n) - \sum_{i=0}^{M-1} s_i \mathbf{W}^T(n-i) \mathbf{X}(n-i) \right] \\
&\quad + 2\gamma y_s(n) \sum_{j=0}^{M-1} \frac{\partial}{\partial \mathbf{W}(n-j)} \left[ \sum_{i=0}^{M-1} s_i \mathbf{W}^T(n-i) \mathbf{X}(n-i) \right] \tag{A2}
\end{aligned}$$

Thus,

$$\begin{aligned}
\sum_{j=0}^{M-1} \frac{\partial J(n)}{\partial \mathbf{W}(n-j)} &= -2[e(n) - \gamma y_s(n)] \sum_{j=0}^{M-1} \frac{\partial}{\partial \mathbf{W}(n-j)} \left[ \sum_{i=0}^{M-1} s_i \mathbf{W}^T(n-i) \mathbf{X}(n-i) \right] \\
&= -2[e(n) - \gamma y_s(n)] \sum_{j=0}^{M-1} s_j \mathbf{X}(n-j) \tag{A3}
\end{aligned}$$

Substituting (A3) in (7) and using (9) yields

$$\mathbf{W}(n+1) = \mathbf{W}(n) + \mu[e(n) - \gamma y_s(n)] \mathbf{X}_f(n) \tag{A4}$$

Since the coefficients of the secondary path  $\mathbf{S}$  are unknown, we replace  $y_s(n)$  in (A4) with  $\hat{y}_s(n)$  given by (10), yielding (8).

## REFERENCES

1. Kuo SM, Morgan DR. *Active Noise Control Systems: Algorithms and DSP Implementations*. Wiley: New York, 1996.
2. Elliott SJ, Nelson PA. Active noise control. *IEEE Signal Processing Magazine* 1993; **10**:12–35.
3. Nelson PA, Elliott SJ. *Active Control of Sound*. Academic Press: New York, 1995.
4. Costa MH, Bermudez JCM, Bershada NJ. Stochastic analysis of the LMS algorithm with a saturation nonlinearity following the adaptive filter output. *IEEE Transactions on Signal Processing* 2001; **43**(7):1370–1387.
5. Costa MH, Bermudez JCM, Bershada NJ. Stochastic analysis of the filtered-X LMS algorithm in systems with nonlinear secondary paths. *IEEE Transactions on Signal Processing* 2002; **50**(6):1327–1342.
6. Stenger A, Kellerman W. Adaptation of a memoryless preprocessor for nonlinear acoustic echo cancelling. *Signal Processing* 2000; **80**:1747–1760.
7. Hansen C. Active noise control—from laboratory to industrial implementation. In *Proceedings of the National Conference on Noise Control Engineering (NOISE-CON)*, June, PA, U.S.A., 1997; 3–38.

8. Tao G, Kokotovic PV. *Adaptive Control of Systems with Actuators and Sensor Nonlinearities*. Wiley: New York, 1996.
9. Klippel W. Dynamic measurements and interpretation of the nonlinear parameters of electrodynamic loudspeakers. *Journal of Audio Engineering Society* 1990; **38**(12):944–955.
10. Klippel W. Nonlinear large-signal behavior of electrodynamic loudspeakers at low frequencies. *Journal of Audio Engineering Society* 1992; **40**(6):483–496.
11. Darlington P, Xu G. Equivalent transfer functions of minimum output variance mean-square estimators. *IEEE Transactions on Signal Processing* 1991; **39**(7):1674–1677.
12. Mayyas K, Aboulnasr T. Leaky LMS algorithm: MSE analysis for Gaussian data. *IEEE Transactions on Signal Processing* 1997; **45**(4):927–934.
13. Bermudez JCM, Costa MH. Optimum leakage factor for the MOV-LMS algorithm in nonlinear modeling and control systems. In *Proceedings of the 2002 IEEE International Conference on Acoustics, Speech and Signal Processing (ICASSP-02)*, May, Orlando, FL, U.S.A., 2002.
14. Darlington P. Performance surfaces of minimum effort estimators and controllers. *IEEE Transactions on Signal Processing* 1995; **43**(2):536–539.
15. Elliot SJ, Stothers IM, Nelson PA. A multiple error LMS algorithm and its application to the active control of sound and vibration. *IEEE Transactions on Acoustics, Speech, and Signal Processing* 1987; **ASSP-35**(10):1423–1434.
16. Kuo BC. *Automatic Control Systems*. Prentice-Hall International: London, England, 1962.
17. Costa MH, Bermudez JCM, Bershada NJ. The performance surface in filtered nonlinear mean square estimation. *IEEE Transactions on Circuits and Systems—I: Fundamental Theory and Applications* 2003; **50**(3):445–447.
18. Price R. A useful theorem for nonlinear devices having Gaussian inputs. *IRE Transactions on Information Theory* 1958; **IT-4**(2):69–72.
19. Bershada NJ. On error-saturation nonlinearities in LMS adaptation. *IEEE Transactions on Acoustics, Speech, and Signal Processing* 1988; **36**(4):440–452.
20. Samson C, Reddy VU. Fixed point error analysis of the normalized ladder algorithms. *IEEE Transactions on Acoustics, Speech and Signal Processing* 1983; **31**(5):1177–1191.
21. Breining C *et al.* Acoustic echo control: an application of very-high-order adaptive filters. *IEEE Signal Processing Magazine* 1999; **16**(16):42–69.
22. Haykin S. *Adaptive Filter Theory* (4th edn). Prentice-Hall: Englewood Cliffs, NJ, 2002.